



Design and synthesis of novel DFG-out RAF/vascular endothelial growth factor receptor 2 (VEGFR2) inhibitors: 2. Synthesis and characterization of a novel imide-type prodrug for improving oral absorption

Masanori Okaniwa^{a,*}, Takashi Imada^a, Tomohiro Ohashi^a, Tohru Miyazaki^a, Takeo Arita^a, Masato Yabuki^a, Akihiko Sumita^b, Shunichirou Tsutsumi^b, Keiko Higashikawa^a, Terufumi Takagi^a, Tomohiro Kawamoto^a, Yoshitaka Inui^a, Sei Yoshida^a, Tomoyasu Ishikawa^{a,*}

^a Pharmaceutical Research Division, Takeda Pharmaceutical Company Limited, 26-1, Muraoka-Higashi 2-chome, Fujisawa, Kanagawa 251-8555, Japan

^b CMC Center, Takeda Pharmaceutical Company Limited, 17-85, Jusohonmachi 2-chome, Yodogawa-ku, Osaka 532-8686, Japan

ARTICLE INFO

Article history:

Received 25 April 2012

Revised 4 June 2012

Accepted 5 June 2012

Available online 15 June 2012

Keywords:

RAF

VEGFR2

Imide-type prodrug

Oral absorption

ABSTRACT

As an alternative to the previously reported solid dispersion formulation for enhancing the oral absorption of thiazolo[5,4-*b*]pyridine **1**, we investigated novel *N*-acyl imide prodrugs of **1** as RAF/vascular endothelial growth factor receptor 2 (VEGFR2) inhibitors. Introducing *N*-acyl promoieties at the benzanilide position gave chemically stable imides. *N*-*tert*-Butoxycarbonyl (Boc) introduced imide **6** was a promising prodrug, which was converted to the active compound **1** after its oral administration in mice. Cocrystals of **6** with AcOH (**6b**) possessed good physicochemical properties with moderate thermodynamic solubility (19 µg/mL). This crystalline prodrug **6b** was rapidly and enzymatically converted into **1** after its oral absorption in mice, rats, dogs, and monkeys. Prodrug **6b** showed *in vivo* antitumor regressive efficacy (*T/C* = −6.4%) in an A375 melanoma xenograft model in rats. Hence, we selected **6b** as a promising candidate and are performing further studies. Herein, we report the design, synthesis, and characterization of novel imide-type prodrugs.

© 2012 Elsevier Ltd. All rights reserved.

1. Introduction

In a previous report¹, we described the synthesis and potent activity of 2-chloro-3-(1-cyanocyclopropyl)-*N*-[5-({2-[(cyclopropylcarbonyl)amino][1,3]thiazolo[5,4-*b*]pyridin-5-yl)oxy}-2-fluorophenyl]benzamide **1** as a RAF/vascular endothelial growth factor receptor 2 (VEGFR2) inhibitor. Compound **1** possesses potent BRAF(V600E) inhibitory activity (*IC*₅₀ = 7.0 nM) and VEGFR2 inhibitory activity (*IC*₅₀ = 2.2 nM). Since **1** showed insufficient solubility and an oral absorption profile, the solid dispersion (SD) formulation technique² was applied to maximize the oral bioavailability of this compound. The SD formulation of this compound (**1-SD**) demonstrated potent antitumor efficacy (*T/C* = −7.0%) in an A375 human melanoma xenograft model in rats based on the improved solubility.

Abbreviations: ¹H NMR, proton nuclear magnetic resonance; AUC, area under the blood concentration/time curve; ERK, extracellular signal-regulated kinase; MC, methylcellulose; MEK, mitogen-activated protein kinase; PK, pharmacokinetic; VEGFR2, vascular endothelial growth factor receptor 2.

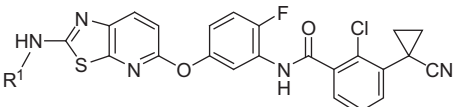
* Corresponding authors. Tel.: +81 466 32 1158; fax: +81 466 29 4449 (M.O.); tel.: +81 466 32 1155; fax: +81 466 29 4449 (T.I.).

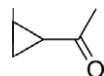
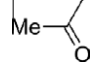
E-mail addresses: masanori.okaniwa@takeda.com (M. Okaniwa), tomoyasu.ishikawa@takeda.com (T. Ishikawa).

Prodrug strategies other than the aforementioned formulation technique have also been utilized for enhancing oral absorption.^{3–5} According to these studies, an important point in prodrug research is choosing the suitable promoiety that must be rapidly cleaved by the enzymes in the body so that a bioactive compound is released after oral administration. Additionally, in most cases, solubility is a significant factor in achieving favorable oral absorption profiles.⁵ However, the choice of the promoiety is often limited and depends on the substructure of the active compounds. For instance, when active compounds possess hydroxy or carboxylic acid groups, the promoieties such as alkoxy carbonates^{6,7} or phosphates⁸ have been used. When active compounds possess amino groups or basic azoles, the promoieties such as phosphono functionalities have been utilized.^{9–11} However, very few studies have reported the introduction of acyl groups onto the amide NH.^{12,13}

Compound **1** possesses cyclopropanecarboxamide and benzanilide groups as amide substructures, and both these functional groups are significant for its potent RAF/VEGFR2 inhibitory activity. In our optimization studies performed on 2-carboxamide groups, cyclopropanecarboxamide **1** was selected because it was stable against hydrolysis by human liver microsomes (Table 1). However, acetamide **2** was comparatively less stable and under-

Table 1
Profiles of [1,3]thiazolo[5,4-*b*]pyridine-2-acylamide **1**, **2**



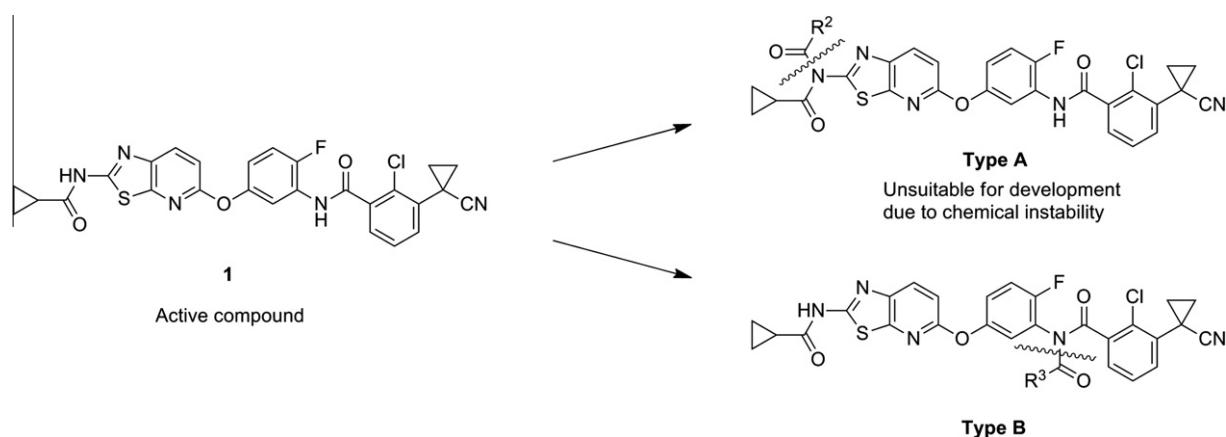
R ¹	Kinase IC ₅₀ ^a (nM)		Cellular pMEK ^b IC ₅₀ (nM)	In vitro hydrolysis ^c	
	BRAF (V600E)	VEGFR2		Unchanged form	Remaining (%)
	7.0 (6.0–8.3)	2.2 (2.0–2.4)	25	109.5	2.4
	6.3 (5.8–6.9)	3.4 (3.1–3.7)	34	78.5	34.6

^a *n* = 2. 95% confidence index values.

^b Concentration producing 50% inhibition (IC₅₀) against Raf substrate MEK phosphorylation in HT-29 (BRAF^{V600E} mutant) cultured human colon cancer cell lines.

^c In vitro hydrolysis stability of each compound (30 μM) was examined using human liver microsomes (1 mg protein/mL). Incubation was carried out for 60 min at 37 °C.

^d Metabolite **3** was identified as a 2-amino derivative (R¹ = H).



went hydrolysis to give the deacetylated [1,3]thiazolo[5,4-*b*]pyridine-2-amine **3** (R¹ = H) as a major metabolite.¹ Under these conditions, the benzanilide moieties of **1** and **2** were very stable, and no cleaved metabolite of benzanilide was observed.

On the basis of the results of in vitro hydrolysis studies by human liver microsomes, we hypothesized that introduction of an enzymatically unstable acyl moiety into **1** may produce a unique imide-type prodrug of **1**. Thus, we designed type **A** possessing an acyl group R² in the cyclopropanecarboxamide moiety and type **B** with an acyl group R³ in the benzanilide moiety (Fig. 1). An initial synthetic investigation found that type **A** compounds were not suitable for development because imide structure of type **A** was chemically too unstable to be isolated in general purification method (see Section 2). Therefore, our research focused on type **B** imide compounds. To evaluate acyl groups for the imide-type prodrug **B**, we screened the following: an enzymatically unstable acetyl group, a cyclopropanecarbonyl group and ethoxycarbonyl and *tert*-butoxycarbonyl (Boc) groups, which afforded carbamate-type derivatives. For an asymmetric bis-acyl imide prodrug **B** with two different acyl groups, it is necessary to consider the regioselectivity of the enzymatic cleavage reaction. The original benzanilide group of the bioactive compound **1** must be more stable than the additional acyl groups.

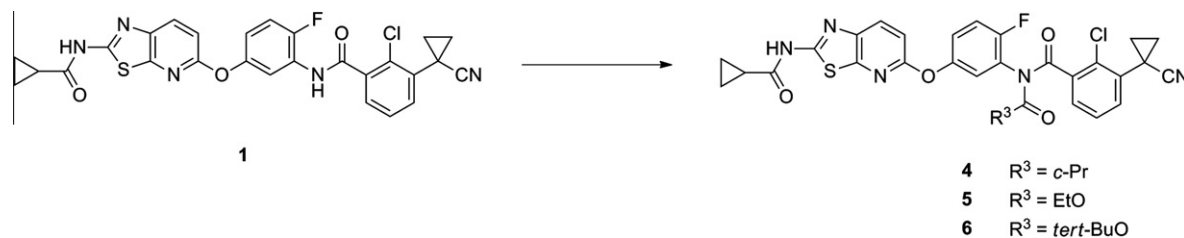
The purpose of this study was the synthesis and evaluation of novel imide-type prodrugs to improve the oral absorption of **1** and the evaluation of the physicochemical and biological profiles of these compounds.

2. Chemistry

Acetylation of **1** was initially examined, but nearly all the reaction conditions afforded complex mixtures inseparable by conventional silica gel column chromatography. Since **1** or the resulting acetylated compounds appeared to be highly sensitive to the reaction conditions used, we attempted the cyclopropanecarbonylation of **1** using cyclopropanecarbonyl chloride, which is less reactive than acetyl chloride. As expected, the cyclopropanecarbonylation of **1** proceeded in the presence of DMAP in pyridine, and type **B** imide product **4** was isolated in 63% yield in a regioselective manner (Scheme 1). The chemical structure of **4** was determined by ¹H NMR and mass spectroscopic analysis. Further, **4** was obtained as chemically stable crystals, as confirmed by powder X-ray diffractometry.

Next, we examined introduction of ethoxycarbonyl group and Boc group into **1**. Ethoxycarbonylation of **1** with diethyl dicarbonate in pyridine afforded the ethoxycarbonylated compound **5** in 45% yield after conventional synthesis and purification by silica gel column chromatography. The Boc group was introduced into **1** by following the similar procedure for ethoxycarbonylation to give **6** in 63% yield. The chemical structures of **5** and **6** corresponded to that of type **B**, and these compounds were also obtained as chemically stable crystals in a regioselective manner.

To clarify the mechanism of regioselective monoacylation, we performed Boc-introducing reaction of **1** in tetrahydrofuran through the stepwise addition of di-*tert*-butyl dicarbonate (Boc₂O)



Scheme 1. Synthesis of type **B** imide compounds **4–6**. Reagents and conditions: (For **4**) cyclopropanecarbonyl chloride (5.2 equiv), DMAP (5.0 equiv), pyridine, room temp, 1.5 h (63%); (For **5**) diethyl dicarbonate (4.9 equiv), pyridine, room temp, 1 h (45%); (For **6**) di-*tert*-butyl dicarbonate (3.0 equiv), pyridine, THF, room temp, 1 h (63%).

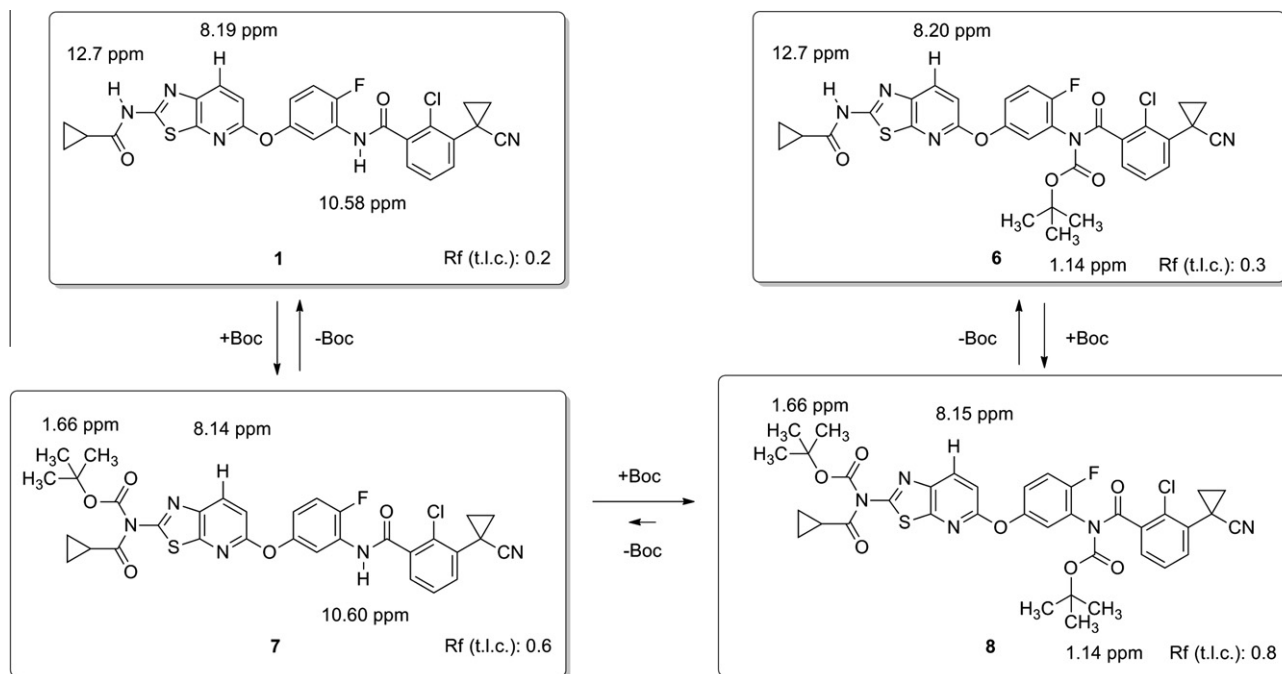


Figure 2. Proposed mechanism of regioselective mono-Boc introduction into **1** for preparing Boc prodrug **6**: reactivity of two amides of **1** and chemical stability of two Boc groups of **8**.

in the presence of pyridine. Without pyridine, this reaction was extremely slow, indicating that pyridine plays a significant role in the activation of amides by deprotonation and/or activation of Boc_2O . In optimal conditions in this reaction, more than 3 equiv of Boc_2O were required to convert **1** to **6** effectively. The results and our proposed mechanism are summarized in Figures 2 and 3. The reaction mixture was monitored by thin-layer chromatography (TLC) and ^1H NMR analysis ($\text{DMSO-}d_6$), in which the aminothiazole amide and benzanilide protons were initially observed with different chemical shifts of 12.7 and 10.58 ppm, respectively (Fig. 3A). The Boc group was first introduced at the aminothiazole amide moiety as type **A**. The formation of a mono-Boc compound **7** was detected by ^1H NMR 30 min after the addition of 1 equiv of Boc_2O . The decrease in the height of the proton peak corresponding to the aminothiazole amide (12.7 ppm) shown in Figure 3B suggested the formation of **7** in the reaction mixture. A singlet peak corresponding to the N-Boc group of aminothiazole imide was also detected at 1.66 ppm. Additionally, the formation of **7** was confirmed by the appearance of an additional spot on the TLC plate (R_f : 0.6 in ethyl acetate/*n*-hexane = 1:1) along with that of the starting material **1** (R_f : 0.2). These results suggested that the reactivity of aminothiazole amide should be higher than that of the benzanilide moiety.

Further monitoring of the reaction revealed a gradual decrease in the intensity of the benzanilide peaks, as shown in Figure 3C, indicating the formation of di-Boc compound **8**. A peak due to the

N-Boc group of benzanilide also appeared at 1.14 ppm. In contrast, the peak due to the aminothiazole amide (12.7 ppm) slowly recovered after 160 min, and four distinguishable doublet peaks were observed in the range 8.14–8.20 ppm. The peaks were considered to be due to the protons at the 4-position of the thiazolo[5,4-*b*]pyridine ring (**1**, **6–8**). Since the produced aminothiazole imides **7** and **8** are reactive intermediates under the reaction conditions employed, we hypothesized that their Boc groups may be transferred to other molecules to assist the “+Boc” reaction. Next, further addition of one equivalent of Boc_2O accelerated the “+Boc” reaction (Fig. 3D). Three equivalents of Boc_2O were necessary for the complete conversion of **1** to **8**, as shown in Figure 3E. In the work up process using hydrochloric acid, selective Boc cleavage occurred at the labile aminothiazole imide position to produce the desired mono-Boc compound **6** (R_f : 0.3) in a regioselective manner (Fig. 3F). We confirmed that this regioselective cleavage also occurred while purifying a crude material by silica gel column chromatography. Based on these results, it was found that the regioselectivity of this mono-acylation was achieved by a cleavage reaction of the labile aminothiazole imide in di-acylated compound.

[1,3]Thiazolo[5,4-*b*]pyridine acetamide derivative **2** and its metabolite **9** (vide infra) were prepared using the route described in Scheme 2. The reaction of commercially available 2-chloro-5-nitropyridine **10** with 3-amino-4-fluorophenol in the presence of potassium carbonate gave the phenoxyated compound **11** in 79%

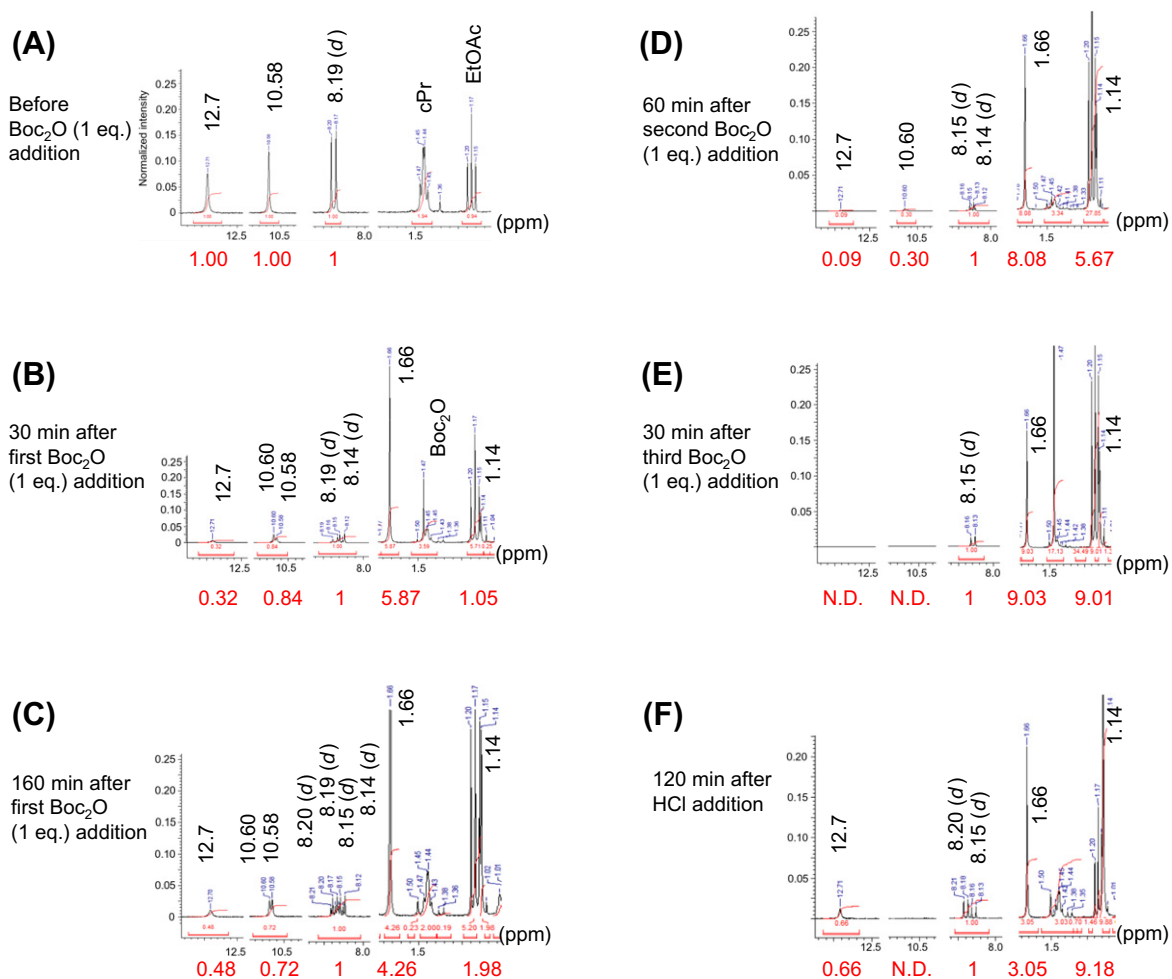
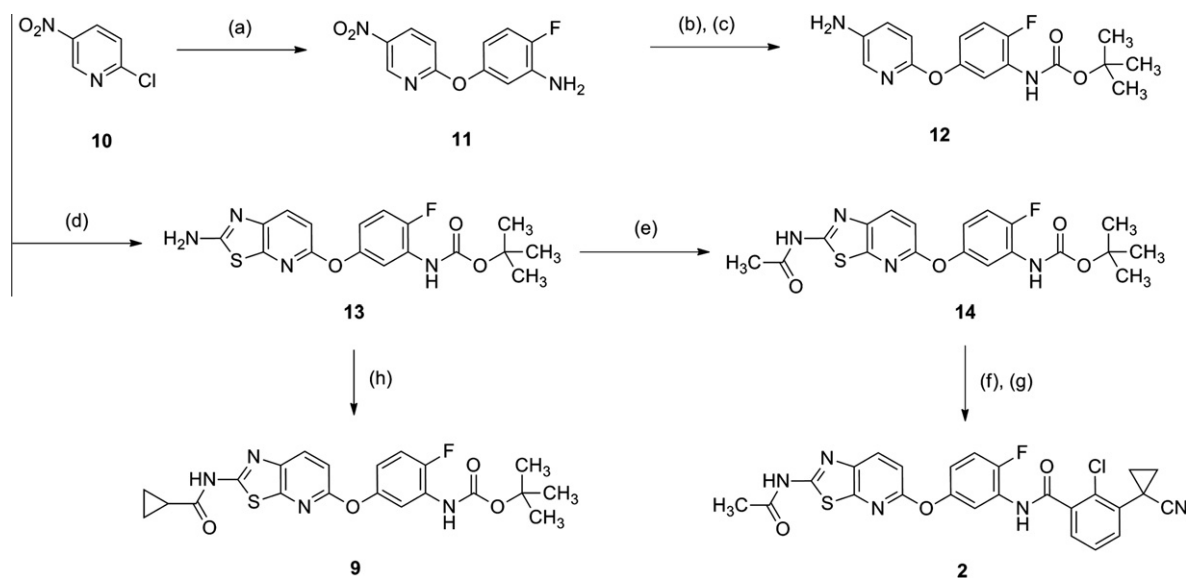
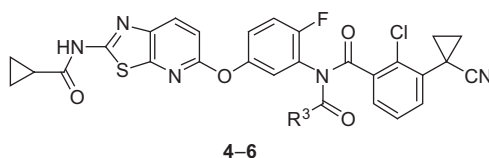


Figure 3. Selected proton signals in ¹H NMR analysis of reaction mixture (A–F). Representative chemical shifts (ppm) are described in black letters; the sum of integrals for the doublet due to C–H at the 4-position of thiazolo[5,4-*b*]pyridines (8.14–8.20 ppm) is set as 1 for the standard.



Scheme 2. Synthesis of [1,3]thiazolo[5,4-*b*]pyridine 2 and 9. Reagents and conditions: (a) 3-amino-4-fluorophenol, K₂CO₃, DMF, room temp, 12 h (79%); (b) Boc₂O, THF, reflux, 12 h (90%); (c) H₂, 10% Pd/C, MeOH, THF, room temp, 12 h (94%); (d) KSCN, Br₂, AcOH, room temp, 12 h (90%); (e) acetyl chloride, pyridine, room temp, 12 h (52%); (f) TFA, room temp, 30 min; (g) 2-chloro-3-(1-cyanocyclopropyl)benzoic acid, COCl₂, cat. DMF, room temp, 30 min (58%); (h) cyclopropanecarbonyl chloride, DMAP, pyridine, room temp, 12 h (59%).

Table 2
Physicochemical properties and mouse PK profiles of imide-type prodrugs **4–6**



R ³	Crystallinity ^a (%)	Melting point ^b (°C)	Solubility ^c (μg/mL)	Mouse PK AUC _{0–8 h} ^d (μg h/mL)	
				Active compound 1	Prodrug intact
4	69	190	3.2	0.511	n.d. ^e
5 EtO	74	220	0.79	0.097	–
6 <i>tert</i> -BuO	44	134 (dec.) ^f	49	4.183	0.062

^a Determined using powder X-ray diffractometry.

^b Determined using differential scanning calorimetry.

^c The Japanese Pharmacopoeia 2nd fluid for disintegration test (pH 6.8) (JP2) containing 20 mmol/L of bile acid.

^d Cassette dosing of five compounds. Values shown are mean ± SD of data from three mice. Compounds (10 mg/kg) were administered in 0.5% methylcellulose in distilled water.

^e Not detected.

^f Decomposition.

Table 3
Physicochemical properties of active compound **1** and *N*-Boc prodrug crystals **6a–b**

	Solvate	Solid form	Crystallinity ^a (%)	Melting point ^b (°C)	Solubility ^c (μg/mL)	Initial dissolution rate ^d (μg/mm ² /min)
1	Solvent free	Crystal	55	213	3.6	0.043
6	Monohydrate	Semicrystal	44	134 (dec.) ^f	49	n.d.
6a	Ethanol (1/1) ^e	Crystal	76	138 (dec.) ^f	4.2	0.072
6b	Acetic acid (1/1) ^e	Crystal	77	141 (dec.) ^f	19	0.101

^a Determined using powder X-ray diffractometry.

^b Determined using differential scanning calorimetry.

^c The Japanese Pharmacopoeia 2nd fluid for disintegration test (pH 6.8) (JP2)¹⁶ containing 20 mmol/L of bile acid.

^d The initial dissolution rates were measured using rotating disk method.

^e Theoretical number of cosolvent was determined by single crystal analysis and described in parenthesis (host/solvate).

^f Decomposition.

yield. Boc protection of the anilino group of **11** (90% yield) and subsequent reduction of the nitro group under conventional hydrogenation conditions afforded the aminopyridine derivative **12** in 94% yield. Cyclization of **12** with potassium thiocyanate and bromine afforded [1,3]thiazolo[5,4-*b*]pyridine-2-amine derivative **13** in 90% yield. Acylation of the 2-amino group of **13** with acetyl chloride in pyridine gave **14** in 52% yield. Cleavage of the *N*-Boc group of **14** using trifluoroacetic acid and subsequent acylation of the resulting amino group with 2-chloro-3-(1-cyanocyclopropyl)benzoic acid¹ under standard conditions provided the desired acetamide **2** in 58% yield in 2 steps.

Metabolite **9** was synthesized in 59% yield by acylation of **13** with cyclopropanecarbonyl chloride in the presence of DMAP in pyridine.

3. Results and discussion

3.1. Physicochemical properties and mouse PK profiles of imide-type prodrugs

Physicochemical properties and mouse PK profiles of synthesized imide compounds **4–6** are summarized in Table 2. After oral administration of 10 mg/kg of cyclopropanecarbonylated imide **4** in mice, the bioactive compound **1** was observed to have an AUC value of 0.511 μg h/mL. In this study, intact compound **4** was not

detected in the blood. Although the solubility (3.2 μg/mL) and oral absorption level of **4** were insufficient, these results motivated the evaluation of other imide-type compounds **5** and **6**. The Boc derivative **6** showed better solubility (49 μg/mL) than did the ethoxycarbonyl derivative **5** (0.79 μg/mL). From our previous investigation, we asserted that modification of the benzanilide substructure of **1** had a significant impact on its solubility.¹ Intro-

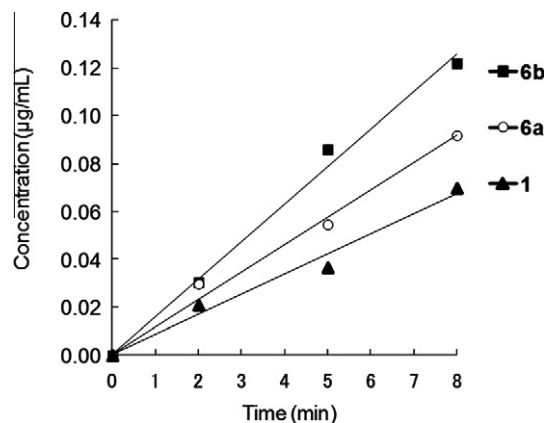


Figure 4. Initial dissolution rate^d of active compound **1** and prodrug **6a–b**. ^gJP2¹⁶ containing 200 mmol/mL of bile acid was used as a solvent.

duction of a chlorine atom into the *ortho*-position of the benzoyl moiety enhanced the solubility by twisting the planar conformation of the benzanilide. In this prodrug research, the introduction of an *N*-Boc group into benzanilide moiety was reflected in a decreased melting point for **6** (mp = 134 °C) as compared to that of the active compound **1** (mp = 213 °C), which implied a decrease in crystal packing energy. We assumed that the bulky lipophilic *tert*-butyl group interferes with intermolecular hydrogen bonding or π - π stacking interactions, thereby decreasing the crystal packing energy and increasing the solubility.¹⁴

Because of the enhanced solubility, the exposure of **1** was dramatically improved (AUC 4.183 $\mu\text{g h/mL}$) in a pharmacokinetic (PK) study after oral administration (dose: 10 mg/kg) of **6** in mice. In this study, the uncleaved, intact **6** was observed to have a low AUC value (0.062 $\mu\text{g h/mL}$). These results suggest that the Boc pro-moiety of **6** is rapidly cleaved after oral absorption and that **6** functions effectively as a prodrug of **1**.

For further evaluation, we conducted a polymorph study of prodrug **6**, which was initially crystallized as a monohydrate from 90% MeOH in H₂O. The crystallinity of **6** remained low (44%), and the

crystals of **6** were considered to be semicrystalline. Hence, we varied the crystallization solvents in order to obtain stable crystals. However, despite numerous crystallization trials, no stable unsolvated crystals were obtained. Some stable solvated cocrystals were obtained when using EtOH, AcOH, acetone, DMSO, and *i*-PrOH. For the pharmaceutical use, residual solvents must be controlled for the safety of drugs. Thus, we selected cocrystals with EtOH (**6a**) and AcOH (**6b**) for further physicochemical evaluation based on the guidelines for residual solvents by the International Conference on Harmonization (ICH).¹⁵

We summarized the physicochemical properties of the prodrug cocrystals of **6a** and **6b** and compared these properties with those of the solvent-free monohydrate **6** and bioactive compound **1**, as shown in Table 3. Both **6a** and **6b** showed sufficient crystallinities of 76% and 77%, respectively. However, the solubility of **6b** (19 $\mu\text{g/mL}$) was significantly higher than that of **6a** (4.2 $\mu\text{g/mL}$).

Next, we compared the dissolution rates of active compound **1** and prodrugs **6a,b** using the Japanese Pharmacopoeia 2nd fluid for disintegration test (pH 6.8) (JP2)¹⁶ containing 200 mmol/mL of bile acid, as shown in Figure 4. As expected, initial dissolution rates of

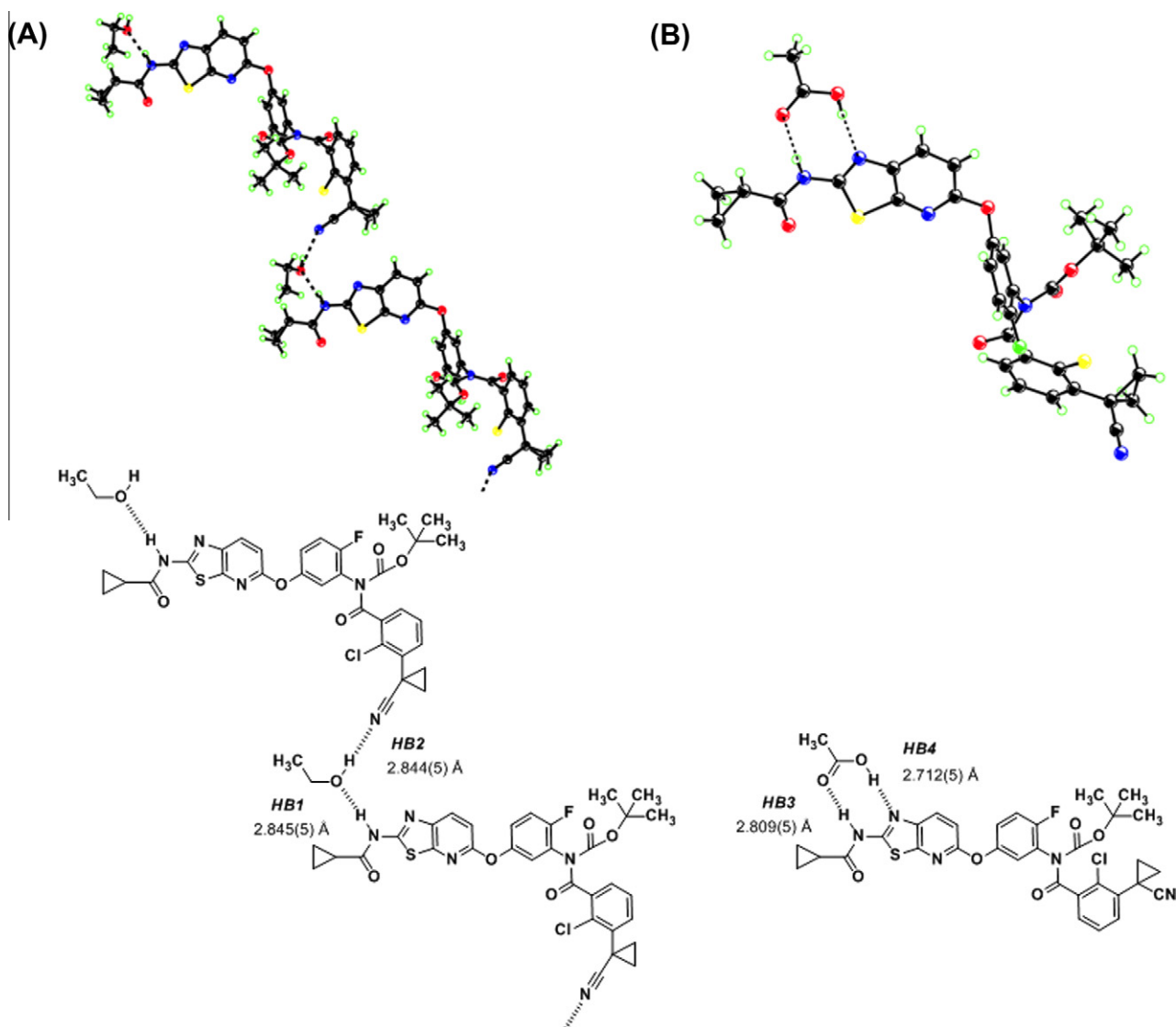


Figure 5. Binding mode of cocrystals determined using single-crystal X-ray structure analysis. Presumed hydrogen bonds (HB) are shown as dotted lines. Numeric data express the hydrogen bond distance (Å) between the donor (D) and acceptor (A) atoms with estimated standard deviations in parentheses. (A) Ethanol cocrystals **6a** (CCDC 862986). The ethanol molecule forms two hydrogen bonds (HB1,2) with two adjacent host molecules. (B) AcOH cocrystals **6b** (CCDC 863435). The AcOH molecule forms two hydrogen bonds (HB3,4) with a single host molecule.

6a (0.072 $\mu\text{g}/\text{mm}^2/\text{min}$) and **6b** (0.101 $\mu\text{g}/\text{mm}^2/\text{min}$) were slightly better than that of **1** (0.043 $\mu\text{g}/\text{mm}^2/\text{min}$). We suspected that the enhanced dissolution rate of **6b** would be reflected by the improved oral absorption of **1** after oral administration of **6b**.

3.2. Single-crystal X-ray structural analysis of **6a** and **6b**

Although we confirmed the enhanced solubility and initial dissolution rate of **6b**, we could not clarify how the physicochemical properties of **6a** (with EtOH) and **6b** (with AcOH) were different. Thus, we conducted single-crystal X-ray structural analysis of the cocrystals of **6a** and **6b** to compare the structural differences between these two compounds, as shown in Figure 5.¹⁷

The cocrystal structure of **6a** (Fig. 5A) shows that the EtOH molecule functions as a hub of intermolecular interaction for **6**. The hydroxy group of EtOH is within the hydrogen bonding distance between two adjacent host molecules of **6** and coordinates two hydrogen bonds, *HB1* and *HB2*, with **6**. The *HB1* and *HB2* distances are 2.845 and 2.844 Å, respectively. Interestingly, these hydrogen bond networks connect each crystal lattice.

However, the cocrystal structure of **6b** (Fig. 5B) shows that the AcOH molecule is located near the aminothiazole moiety and forms bidentate hydrogen bonds (*HB3* and *HB4*) with a single host molecule **6**. The *HB3* and *HB4* distances are 2.809 and 2.712 Å, respectively. The hydrogen bond network in **6b** does not extend beyond the crystal lattice, as opposed to that in **6a**. The solubility and dissolution rate of **6b** are higher than those of **6a** because of the lower crystal lattice energy of the former. Thus, we assume that the hydrogen bond networks of the synthon connect to each other in **6a** with increased crystal lattice energy, thus negatively impacting the solubility of **6a**. However, the crystal motif of **6b** may be advantageous for dissolution because there are no hydrogen bonds between the synthons.

In the cocrystal structure of **6b**, the distances between hydrogen and the donor oxygen (D–H), and hydrogen and the acceptor azole (H...A) were measured using discrete Fourier transform analysis, as shown in Figure 6. Although an observed D–H distance of 1.151 Å was slightly longer than a typical O–H bond length (1.015 Å) in carboxylic acids,¹⁸ the hydrogen atom was observed near the donor oxygen atom as compared to a distance of 1.563 Å from the acceptor nitrogen atom. These results suggest

that the AcOH molecule in **6b** should exist in the un-ionized molecular form. This indicates that **6b** is not a salt but an AcOH solvate.

3.3. In vivo biological profiles of imide-type prodrug **6b**

The selected prodrug **6b** was evaluated by in vivo testing in a human melanoma A375 xenograft model in rats. The prodrug **6b** showed a dose-dependent inhibitory activity against phosphorylation of downstream ERK1/2 (pERK1/2) 4 h after treatment at doses of 12.9, 32.3, and 129 mg/kg, as shown in Figure 7A, which are equivalent to doses of 10, 30, and 100 mg/kg of **1**. On the basis of these results, we performed anti-tumor efficacy studies with twice-daily oral administration in rats (Fig. 7B). Reflecting the pERK1/2 inhibitory effects, **6b** exhibited potent anti-tumor efficacy at a dose of more than 32.3 mg/kg (30 mg/kg as **1**) in a dose-dependent manner. Interestingly, at a dose of 129 mg/kg (100 mg/kg as **1**), **6b** demonstrated tumor regression efficacy (T/C: –6.4%) without severe body weight loss.

3.4. Pharmacokinetic profiles of prodrug **6b** in various animals

To further evaluate **6b** as a prodrug of **1**, PK profiles were investigated in various animals (Table 4). In these studies, the active compound **1** was the main product in all the animals. Nearly all of **6b** was converted into **1**, but a minor amount of metabolite **9** was also observed. For example, at a dose of 64.6 mg/kg in nude rats, **9** was detected and found to have an AUC value of 1.80 $\mu\text{g h/mL}$. In this experiment, the exposure of active compound **1** was $\text{AUC}_{0-24\text{ h}} 4.28 \mu\text{g h/mL}$. In view of the weak BRAF inhibitory activity ($\text{IC}_{50} = 2000 \text{ nM}$) of metabolite **9**, we reasoned that the antitumor efficacy based on pERK inhibition shown in Figure 7 should be mainly derived from the treatment of active compound **1** released from prodrug **6b**.

Furthermore, it was found that **6b** functions more effectively as a prodrug of **1** in dogs and monkeys than in rats. The efficacious AUC values for **1** were 25.33 and 9.90 $\mu\text{g h/mL}$ in dogs and monkeys, respectively. Interestingly, the production levels of the undesired metabolite **9** were low in these non-rodent animals. The 40 and 330-times higher ratio of AUC values of **1** against that of **9** were achieved in dogs and monkeys, but in rats the ratio was only 2.4 times. These results revealed that the cleavage ratio of the

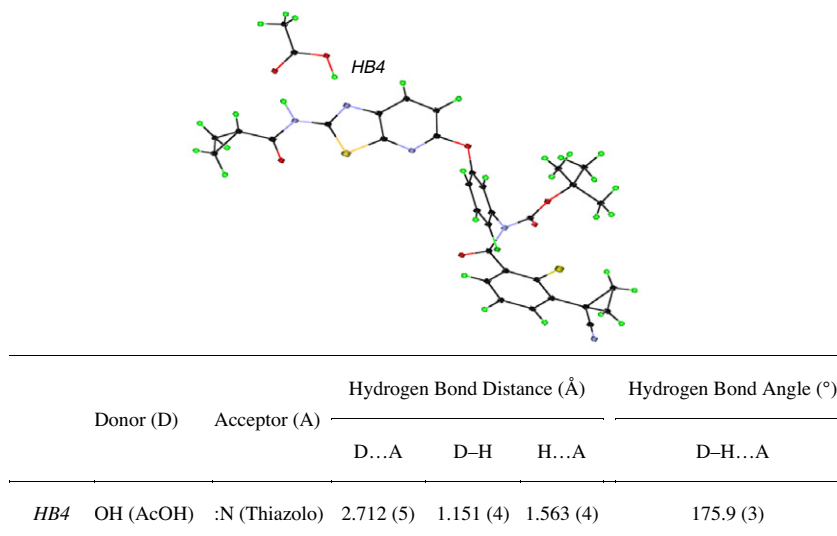


Figure 6. Single crystal structure of **6b** with AcOH, showing hydrogen peaks (light green) observed after discrete Fourier transformation.

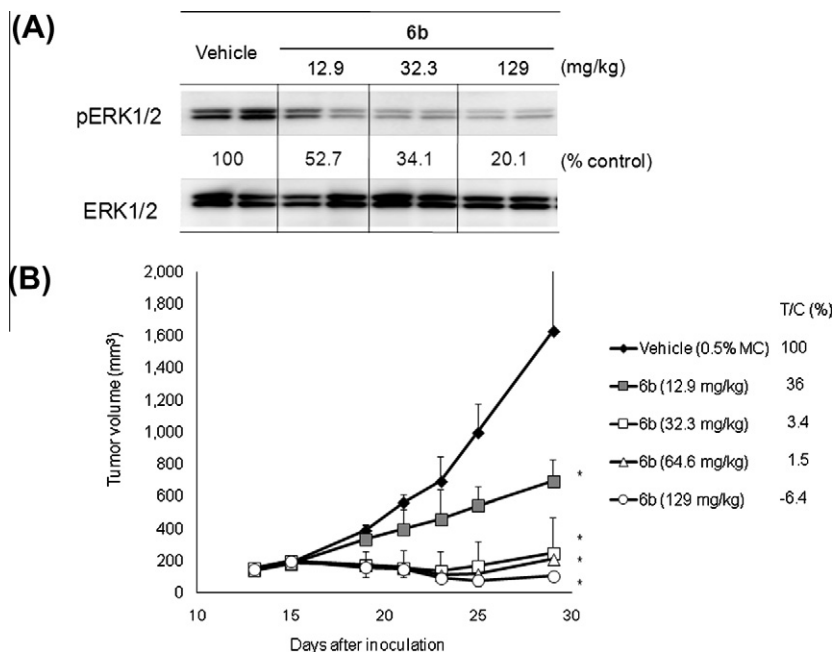


Figure 7. In vivo studies of **6b** in A375 human melanoma xenograft models in F344 nude rats. (A) Mean phosphorylated ERK1/2 levels in tumor tissues were detected ($n = 2$) 4 h after treatment with a single dose. (B) Mean tumor volumes were determined ($n = 4$); $P \leq 0.025$ versus control at day 14 (Shirley–Williams test).

imide-type prodrug **6b** is species-dependent, but the cleavage reaction primarily produced the desired bioactive compound **1** in these selected animals.

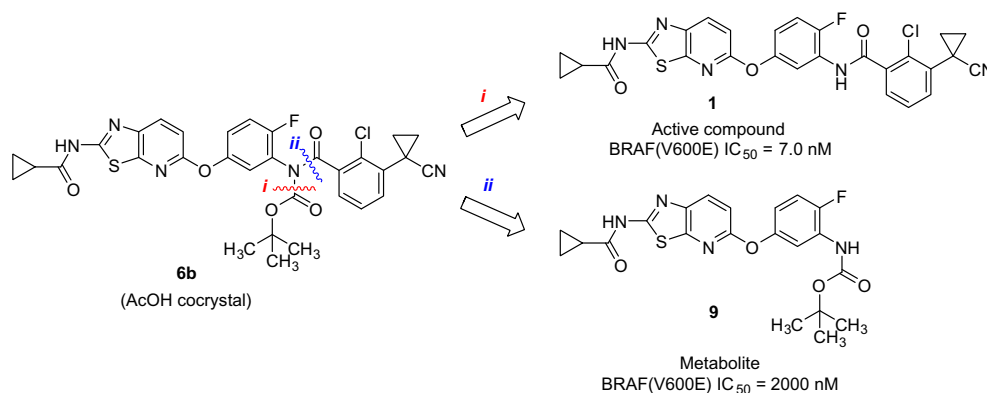
To investigate the differences among various species and predict human PK profiles, we examined the in vitro metabolism using hepatic microsomes, as shown in Table 5. In rodents, the in vitro formation of **9** was comparable to that of **1** in rats

(ratio of formation **1/9** = 0.76), but the latter was dominantly formed in mice (ratio of formation **1/9** = 19). Prodrug **6b** was converted into **1** in dogs (ratio = 3.3) and monkeys (ratio = 3.0). Notably, in humans, prodrug **6b** selectively produced **1** with a ratio of 152.

A comparison of the ratio of in vitro formation and in vivo AUC is shown in Figure 8. Since the AUC ratios were generally higher

Table 4

Selected oral pharmacokinetic profiles of **6b** in various animals



Species	Dose (mg/kg)	AUC _{0–24 h} (μg h/mL) ^a			Ratio AUC _{0–24 h} 1/9
		Prodrug 6	Active compound 1	Metabolite 9	
Mice	32.3 ^b	0.37 ± 0.06	4.90 ± 1.56	0.50 ± 0.17	9.8
Rats (Nude)	12.9 ^b	0.02 ± 0.00	1.39 ± 0.30	0.57 ± 0.06	2.4
Rats (Nude)	64.6 ^b	0.08 ± 0.02	4.28 ± 1.03	1.80 ± 0.24	2.4
Dogs	32.3 ^b	0.53 ± 0.12	25.33 ± 4.11	0.63 ± 0.23	40
Monkeys	32.3 ^b	0.53 ± 0.23	9.90 ± 3.52	0.03 ± 0.06	330

^a Values shown are mean ± SD of data from three animals.

^b Delivered in 0.5% methylcellulose in distilled water.

Table 5
Difference in the formation of active compound **1** and metabolite **9** from prodrug **6b** by hepatic microsomes between different species

Species	In vitro formation ^a		
	Active compound 1 formation (%)	Metabolite 9 formation (%)	Ratio 1/9
Mice	52.3	2.8	19
Rats	15.3	20.2	0.76
Dogs	2.3	0.7	3.3
Monkeys	1.8	0.6	3.0
Humans	15.2	0.1	152

^a Hepatic microsomes (4 mg protein/mL) and **6b** (10 μmol/L) were used. Reactions were carried out at 37 °C for 2 h.

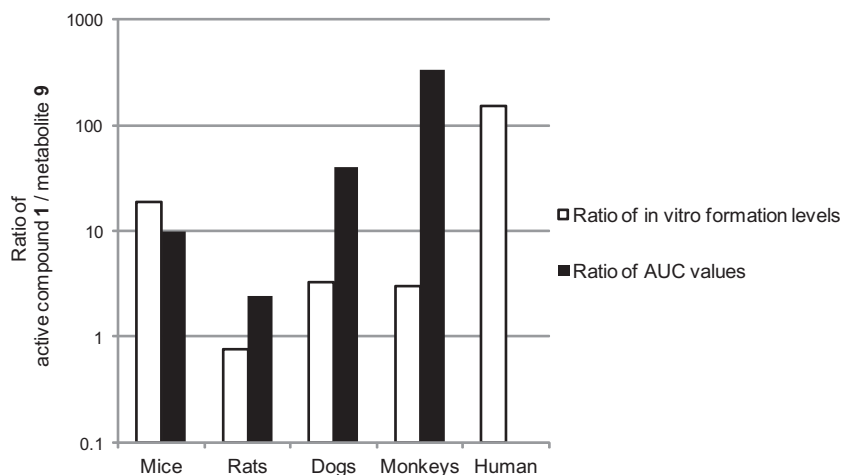


Figure 8. Comparison of ratio between in vitro formation levels by microsome and AUC values in various animals.

than those in a hepatic microsomal study performed on rats, dogs, and monkeys, PK in humans for **6b** may be a promising as the prodrug of the active compound **1**.

4. Conclusion

To enhance the oral absorption of active compound **1**, we designed and investigated novel *N*-acyl imide-type prodrugs. We found that an *N*-acyl promoiety introduced at the benzanilide position provided chemically stable type **B** imides. Particularly, introduction of *N*-Boc into the imide **6** resulted in significant improvement of the solubility and oral absorption in mice. Furthermore, cocrystals of **6b** with AcOH had good physicochemical properties with moderate thermodynamic solubility (19 μg/mL) and showed potent in vivo antitumor regressive efficacy ($T/C = -6.4\%$) in a human melanoma A375 xenograft model in rats based on the potent BRAF(V600E) inhibitory activity of **1** ($IC_{50} = 7.0$ nM). As discussed in our previous reports, the antitumor efficacy of the prodrug of **1** was thought to include the additional efficacy derived from the potent VEGFR2 inhibitory activity of **1** ($IC_{50} = 2.2$ nM). Pharmacokinetics studies on **6b** in various animals showed that this compound functions effectively as a prodrug of **1** in dogs and monkeys than in rats.

Thus, we conclude that the Boc-introduced imide compound practically functions as a prodrug for improving thermodynamic solubility and oral absorption, and prodrug **6b** is a promising candidate for a RAF/VEGFR2 inhibitor.

5. Experimental section

5.1. General chemistry information

The starting materials, reagents, and solvents were reagent-grade and used as purchased. Thin-layer chromatography (TLC)

was carried out using Merck Kieselgel 60, 63–200 mesh, F254 plates or Fuji Silysia Chemical Ltd, 100–200 mesh, NH plates. Chromatographic purification was carried out using silica gel (Merck, 70–230 mesh) or basic silica gel (Fuji Silysia Chemical Ltd, DM1020, 100–200 mesh). Melting points were obtained using an OptiMelt melting point apparatus MPA100 and used uncorrected. Proton nuclear magnetic resonance (¹H NMR) spectra were obtained using a Bruker AVANCE II (300 MHz) spectrometer with tetramethylsilane (TMS) as the internal standard. The data are given as follows: chemical shift (δ) in ppm, multiplicity (where applicable), coupling constants (J) in Hz (where applicable), and integration (where applicable). Multiplicities are indicated by s (singlet), d (doublet), t (triplet), q (quartet), dd (double doublet), br s (broad singlet), or m (multiplet). MS spectra were collected with a Waters LC-MS system (ZMD-1) and were used to confirm $\geq 95\%$ purity of each compound. The column used was an L-column 2 ODS (3.0 × 50 mm I.D., CERI, Japan) with a temperature of 40 °C and a flow rate of 1.2 mL/min. Mobile phase A was 0.05% TFA in ultrapure water. Mobile phase B was 0.05% TFA in acetonitrile which was increased linearly from 5% to 90% over 2 min, 90% over the next 1.5 min, after which the column was equilibrated to 5% for 0.5 min. Elemental analyses (Anal.) and high-resolution mass spectroscopy (HRMS) were carried out at Takeda Analytical Laboratories, Ltd. Yields were not optimized.

5.2. *N*-(5-([2-(Acetylamino)[1,3]thiazolo[5,4-*b*]pyridin-5-yl]oxy)-2-fluorophenyl)-2-chloro-3-(1-cyanocyclopropyl)benzamide (**2**)

A solution of *tert*-butyl (5-([2-(acetylamino)[1,3]thiazolo[5,4-*b*]pyridin-5-yl]oxy)-2-fluorophenyl)carbamate (**14**, 0.65 g, 1.54 mmol) in trifluoroacetic acid (5 mL) was stirred at room temperature for 30 min. The reaction mixture was concentrated under

reduced pressure, and the residue was diluted with ethyl acetate (100 mL), washed with 0.1 N NaOH (100 mL), and dried over anhydrous MgSO₄. The insoluble material was filtered off, and the filtrate was concentrated under reduced pressure. The obtained residue was triturated with diethyl ether to give *N*-[5-(3-amino-4-fluorophenoxy)[1,3]thiazolo[5,4-*b*]pyridin-2-yl]acetamide (0.49 g, quantitative yield) as white amorphous solid. ¹H NMR (DMSO-*d*₆, 300 MHz): δ 2.27 (s, 3H), 4.03 (br s, 2H), 6.40–6.46 (m, 1H), 6.61 (dd, *J* = 3.0, 7.5 Hz, 1H), 6.89 (d, *J* = 8.7 Hz, 1H), 6.97 (dd, *J* = 8.7, 10.8 Hz, 1H), 7.92 (d, *J* = 8.7 Hz, 1H), 11.66 (br s, 1H). HRMS (ESI): calcd for C₁₄H₁₁FN₄O₂S [M+H]⁺ 319.0660. Found: 319.0641.

To a solution of 2-chloro-3-(1-cyanocyclopropyl)benzoic acid¹ (0.33 g, 1.5 mmol) in oxalyl chloride (1.5 mL) was added DMF (100 μL), and the mixture was stirred at room temperature for 30 min, and concentrated to dryness under reduced pressure. This material was dissolved in a mixture of *N,N*-dimethylacetamide/tetrahydrofuran (1:1, 3 mL), and the solution was added dropwise to a solution of *N*-[5-(3-amino-4-fluorophenoxy)[1,3]thiazolo[5,4-*b*]pyridin-2-yl]acetamide (0.33 g, 1.00 mmol) in *N,N*-dimethylacetamide (3 mL) under ice-cooling. The reaction mixture was stirred at room temperature for 3 h, and poured into water (100 mL), and the mixture was extracted with ethyl acetate (2 × 100 mL). The combined organic layers were dried over anhydrous Na₂SO₄. The insoluble material was filtered off, and the filtrate was concentrated under reduced pressure. The obtained residue was purified by silica gel column chromatography (0–100% ethyl acetate/*n*-hexane), and recrystallized from methanol to give **2** (280 mg, 54%) as colorless crystalline solid; mp 213–215 °C. ¹H NMR (DMSO-*d*₆, 300 MHz): δ 1.39 (dd, *J* = 5.1, 7.5 Hz, 2H), 1.82 (dd, *J* = 5.4, 7.5 Hz, 2H), 2.30 (s, 3H), 6.94–6.99 (m, 1H), 7.03 (d, *J* = 8.7 Hz, 1H), 7.19 (dd, *J* = 9.0, 10.5 Hz, 1H), 7.39 (t, *J* = 7.8 Hz, 1H), 7.50 (dd, *J* = 1.8, 7.8 Hz, 1H), 7.68 (dd, *J* = 1.8, 7.8 Hz, 1H), 7.97 (d, *J* = 8.7 Hz, 1H), 8.06 (d, *J* = 3.0 Hz, 1H), 8.39 (dd, *J* = 2.7, 6.6 Hz, 1H), 9.18 (br s, 1H). HRMS (ESI): calcd for C₂₅H₁₇ClFN₅O₃S [M+H]⁺ 522.0797. Found: 522.0803.

5.3. 2-Chloro-3-(1-cyanocyclopropyl)-*N*-(cyclopropylcarbonyl)-*N*-[5-({2-[(cyclopropylcarbonyl)amino][1,3]thiazolo[5,4-*b*]pyridin-5-yl}oxy)-2-fluorophenyl]benzamide (**4**)

To a mixture of compound **1**¹ (3.5 g, 6.39 mmol) and DMAP (3.87 g, 31.7 mmol) in pyridine (35 mL) was added cyclopropane-carbonyl chloride (3.0 mL, 33.1 mmol) at 10 °C. The reaction mixture was stirred at room temperature for 1.5 h. The mixture was poured into cooled water (70 mL), and the mixture was extracted with ethyl acetate (3 × 80 mL). The organic layer was washed with water (50 mL) and brine (30 mL), successively, and dried over anhydrous MgSO₄. The insoluble was filtered off, and the filtrate was concentrated under reduced pressure. The residue was purified by silica gel column chromatography (mesh 60 μm, 100 g, eluent 5–80% ethyl acetate in *n*-hexane). Desired fractions were combined and evaporated under reduced pressure. Crystallization of the residue was carried out from ethyl acetate, and the obtained crystals were collected by filtration, dried under vacuum to give **4** as white crystalline solid (2.47 g, 63%); mp 190 °C. ¹H NMR (DMSO-*d*₆, 300 MHz): δ 0.84–1.03 (8H, m), 1.33–1.44 (m, 2H), 1.72–1.80 (m, 2H), 1.81–1.93 (m, 1H), 1.93–2.06 (m, 1H), 7.13 (d, *J* = 8.7 Hz, 1H), 7.29–7.64 (m, 6H), 8.19 (d, *J* = 8.7 Hz, 1H), 12.71 (br s, 1H). Powder X-ray diffraction (Cu-Kα radiation, diffraction angle: 2θ (°)): 2.52, 2.76, 4.22, 4.86, 5.24, 7.46, 8.46, 9.76, 10.18, 10.54, 11.36, 11.62, 12.38, 13.04, 13.52, 13.84, 14.14, 14.78, 15.28, 15.56, 15.88, 16.32, 16.6, 16.8, 17.34, 17.8, 18.68, 19.12, 19.54, 20.02, 21.02, 21.56, 21.98, 22.7, 22.94, 23.4, 23.8, 24.5, 24.86. Anal. Calcd for C₃₁H₂₃ClFN₅O₄S: C, 60.44; H, 3.76; N, 11.37. Found: C, 60.26; H, 3.84; N, 11.25.

5.4. Ethyl {[2-chloro-3-(1-cyanocyclopropyl)phenyl]carbonyl}[5-({2-[(cyclopropylcarbonyl)amino][1,3]thiazolo[5,4-*b*]pyridin-5-yl}oxy)-2-fluorophenyl]carbamate (**5**)

To a mixture of compound **1** (151 mg, 0.278 mmol) in pyridine (1.5 mL) was added diethyl dicarbonate (197 μL, 1.36 mmol) at room temperature. The reaction mixture was stirred at room temperature for 1 h. To the mixture was added water (5 mL), and the mixture was extracted with ethyl acetate (3 × 5 mL). The organic layer was washed with water (5 mL) and brine (2 mL), successively, and dried over anhydrous MgSO₄. The insoluble was filtered off, and the filtrate was concentrated under reduced pressure. The residue was purified by silica gel column chromatography (mesh 60 μm, 100 g, eluent 5–80% ethyl acetate in *n*-hexane). Desired fractions were combined and evaporated under reduced pressure. Crystallization of the residue was carried out from ethyl acetate, and the obtained crystals were collected by filtration, dried under vacuum to give **5** as white crystalline solid (77.6 mg, 45%); mp 220 °C. ¹H NMR (DMSO-*d*₆, 300 MHz): δ 0.90 (t, *J* = 7.1 Hz, 3H), 0.93–1.00 (m, 4H), 1.39–1.49 (m, 2H), 1.75–1.85 (m, 2H), 1.93–2.06 (m, 1H), 4.03 (q, *J* = 7.1 Hz, 2H), 7.16 (d, *J* = 8.7 Hz, 1H), 7.32–7.40 (m, 1H), 7.43–7.51 (m, 2H), 7.51–7.58 (m, 1H), 7.59–7.70 (m, 2H), 8.19 (d, *J* = 8.7 Hz, 1H), 12.70 (br s, 1H). Powder X-ray diffraction (Cu-Kα radiation, diffraction angle: 2θ (°)): 6.88, 9.68, 10.52, 11.76, 12.62, 13.32, 14.14, 14.54, 14.92. Anal. Calcd for C₃₀H₂₃ClFN₅O₄S: C, 58.11; H, 3.74; N, 11.29. Found: C, 58.10; H, 3.86; N, 11.08.

5.5. *tert*-Butyl {[2-chloro-3-(1-cyanocyclopropyl)phenyl]carbonyl}[5-({2-[(cyclopropylcarbonyl)amino][1,3]thiazolo[5,4-*b*]pyridin-5-yl}oxy)-2-fluorophenyl]carbamate monohydrate (**6**)

To a solution of **1** (3.0 g, 5.47 mmol) in pyridine (55 mL) was added dropwise di-*tert*-butyl dicarbonate (3.58 g, 16.4 mmol) in THF (17 mL) at room temperature. The mixture was stirred at room temperature for 1 h. It was then diluted with water (120 mL) and ethyl acetate (240 mL). The organic layer was washed with brine (120 mL) and dried over anhydrous Na₂SO₄. The insoluble was filtered off, and the filtrate was concentrated under reduced pressure. The residue was purified by silica gel column chromatography (mesh 60 μm, 100 g, eluent 5–80% ethyl acetate in *n*-hexane). Desired fractions were combined and evaporated in vacuo to give crude **6** as white amorphous powder (2.25 g, 63%). Crystallization of the crude **6** (1.0 g) was carried out from methanol/water (9:1, 10 mL), and the obtained crystals were collected by filtration, dried at 75 °C under vacuum to give **6** (0.95 g, 95%) as monohydrate white crystalline solid; mp 134 °C (dec). ¹H NMR (DMSO-*d*₆, 300 MHz): δ 0.84–1.02 (m, 4H), 1.14 (s, 9H), 1.32–1.55 (m, 2H), 1.68–1.88 (m, 2H), 1.90–2.08 (m, 1H), 7.16 (d, *J* = 8.7 Hz, 1H), 7.27–7.40 (m, 1H), 7.42–7.55 (m, 3H), 7.60–7.76 (m, 2H), 8.20 (d, *J* = 8.7 Hz, 1H), 12.70 (s, 1H). Powder X-ray diffraction (Cu-Kα radiation, diffraction angle: 2θ (°)): 2.86, 5.84, 9.90, 10.96, 11.2, 11.64, 12.78, 13.26, 14.9, 15.4, 15.8, 16.56, 17.28, 17.8, 18.46, 18.82, 19.1, 19.98, 20.38, 21.66, 22.02, 22.64, 22.9, 23.12, 23.5, 23.8, 24.78. Anal. Calcd for C₃₂H₂₇ClFN₅O₅·H₂O: C, 57.70; H, 4.39; N, 10.51. Found: C, 57.90; H, 4.39; N, 10.37.

5.6. *tert*-Butyl {[2-chloro-3-(1-cyanocyclopropyl)phenyl]carbonyl}[5-({2-[(cyclopropylcarbonyl)amino][1,3]thiazolo[5,4-*b*]pyridin-5-yl}oxy)-2-fluorophenyl]carbamate ethanol (1/1) solvate (**6a**)

Crystallization of **6** (50 mg) was carried out from ethanol/water (9:1, 0.44 mL), and the obtained crystals were collected by filtration, dried at 75 °C under vacuum to give **6a** (45 mg, 84%) as white

crystalline solid; mp 138 °C (dec). ^1H NMR (DMSO- d_6 , 300 MHz): δ 0.82–1.00 (m, 4H), 1.06 (t, J = 7.0 Hz, 3H), 1.14 (s, 9H), 1.35–1.58 (m, 2H), 1.71–1.85 (m, 2H), 1.94–2.07 (m, 1H), 3.38–3.53 (m, 2H), 4.34 (t, J = 5.1 Hz, 1H), 7.16 (d, J = 8.7 Hz, 1H), 7.26–7.41 (m, 1H), 7.41–7.57 (m, 3H), 7.60–7.74 (m, 2H), 8.19 (d, J = 8.7 Hz, 1H), 12.70 (br s, 1H). Powder X-ray diffraction (Cu-K α radiation, diffraction angle: 2θ (°)): 5.98, 9.76, 10, 11.64, 12.04, 12.98, 13.32, 14.46, 14.78, 15.16, 15.9, 16.56, 16.98, 17.76, 18.16, 18.58, 18.94, 19.32, 19.62, 20.08, 20.42, 20.98, 21.2, 21.46, 22.22, 22.56, 23.28, 23.44, 23.9, 24.32, 24.78. Anal. Calcd for $\text{C}_{32}\text{H}_{27}\text{ClFN}_5\text{O}_5\text{S}$ ·1.0 EtOH·0.5H $_2\text{O}$: C, 58.07; H, 4.87; N, 9.96. Found: C, 57.90; H, 4.73; N, 10.06.

5.7. *tert*-Butyl {[2-chloro-3-(1-cyanocyclopropyl)phenyl]carbonyl}[5-({2-[(cyclopropylcarbonyl)amino][1,3]thiazolo[5,4-*b*]pyridin-5-yl)oxy}-2-fluorophenyl]carbamate acetic acid (1/1) solvate (6b)

Crystallization of **6** (200 mg) was carried out from acetic acid/water (4:1, 1.0 mL), and the obtained crystals were collected by filtration, dried at 60 °C under vacuum to give **6b** (199 mg, 91%) as white crystalline solid; mp 141 °C (dec). ^1H NMR (DMSO- d_6 , 300 MHz): δ 0.85–1.05 (m, 4H), 1.14 (s, 9H), 1.38–1.53 (m, 2H), 1.74–1.85 (m, 2H), 1.90 (s, 3H), 1.94–2.07 (m, 1H), 7.17 (d, J = 8.7 Hz, 1H), 7.28–7.40 (m, 1H), 7.42–7.57 (m, 3H), 7.61–7.73 (m, 2H), 8.20 (d, J = 8.7 Hz, 1H), 11.95–12.93 (br s, 2H). Powder X-ray diffraction (Cu-K α radiation, diffraction angle: 2θ (°)): 6.16, 7.72, 8.4, 8.78, 9.1, 10.84, 11.16, 11.64, 12.44, 12.64, 12.92, 13.38, 13.98, 14.26, 14.58, 15.4, 16.1, 16.42, 17.06, 17.74, 17.98, 18.48, 18.8, 19.72, 20.04, 20.34, 20.72, 21.08, 21.58, 21.92, 22.54, 22.94, 23.62, 24.04, 24.28, 24.82. Anal. Calcd for $\text{C}_{32}\text{H}_{27}\text{ClFN}_5\text{O}_5\text{S}$ ·1.0AcOH: C, 57.67; H, 4.41; N, 9.89. Found: C, 57.58; H, 4.47; N, 9.85.

5.8. *tert*-Butyl (5-{{2-(cyclopropylcarbonyl)amino}[1,3]thiazolo[5,4-*b*]pyridin-5-yl}oxy)-2-fluorophenyl]carbamate (9)

To a solution of *tert*-butyl {5-[(2-amino[1,3]thiazolo[5,4-*b*]pyridin-5-yl)oxy]-2-fluorophenyl}carbamate **13** (1.13 g, 3.0 mmol) and DMAP (1.22 g, 10 mmol) in pyridine (10 mL) was added dropwise cyclopropanecarbonyl chloride (1.05 g, 10 mmol) under ice-cooling, and the reaction mixture was stirred at room temperature for 12 h. To the reaction mixture was added water (200 mL), and the mixture was extracted with ethyl acetate (2 \times 100 mL). The combined organic layers were dried over anhydrous MgSO_4 . The insoluble material was filtered off, and the filtrate was concentrated under reduced pressure. The obtained residue was triturated with diethyl ether to give **9** (0.78 g, 59%) as pale yellow amorphous solid. Crystallization of the solid was carried out from ethyl acetate/*n*-heptane (1:1), and the obtained crystals were collected by filtration, dried under vacuum to give colorless crystalline solid; mp 268–270 °C. ^1H NMR (DMSO- d_6 , 300 MHz): δ 1.02–1.10 (m, 2H), 1.21–1.28 (m, 2H), 1.50 (s, 9H), 1.58–1.67 (m, 1H), 6.76–6.81 (m, 2H), 6.95 (d, J = 8.7 Hz, 1H), 7.08 (dd, J = 9.0, 10.8 Hz, 1H), 7.96 (d, J = 3.6 Hz, 1H), 7.97 (br s, 1H), 10.12 (br s, 1H). MS (ESI): m/z 445 (M+H) $^+$. Anal. Calcd for $\text{C}_{21}\text{H}_{21}\text{FN}_4\text{O}_4\text{S}$: C, 56.75; H, 4.76; N, 12.61. Found: C, 56.51; H, 4.83; N, 12.47.

5.9. 2-Fluoro-5-[(5-nitropyridin-2-yl)oxy]aniline (11)

A mixture of 2-chloro-5-nitropyridine (**10**, 6.34 g, 40 mmol), 3-amino-4-fluorophenol (5.08 g, 40 mmol) and potassium carbonate (5.52 g, 40 mmol) in DMF (20 mL) was stirred at room temperature for 12 h. The reaction mixture was poured into water (200 mL), and the mixture was extracted with ethyl acetate (2 \times 100 mL). The combined organic layers were dried over anhydrous Na_2SO_4 . The insoluble material was filtered off, and the filtrate was concen-

trated under reduced pressure. The obtained residue was purified by silica gel column chromatography (50–100% ethyl acetate/*n*-hexane), and crystallized from diethyl ether. The obtained crystals were collected by filtration, dried under vacuum to give **11** (7.90 g, 79%) as yellow powder. ^1H NMR (DMSO- d_6 , 300 MHz): δ 3.88 (br s, 2H), 6.43–6.48 (m, 1H), 6.57 (dd, J = 2.7, 9.0 Hz, 1H), 6.99 (dd, J = 0.6, 9.0 Hz, 1H), 7.04 (dd, J = 8.7, 10.5 Hz, 1H), 8.46 (dd, J = 3.0, 9.0 Hz, 1H), 9.06 (dd, J = 0.3, 2.7 Hz, 1H). HRMS (ESI): calcd for $\text{C}_{11}\text{H}_8\text{FN}_3\text{O}_3$ [M+H] $^+$ 250.0622. Found: 250.0607.

5.10. *tert*-Butyl {5-[(5-aminopyridin-2-yl)oxy]-2-fluorophenyl}carbamate (12)

A solution of **11** (7.43 g, 30 mmol) and di-*tert*-butyl dicarbonate (10.9 g, 50 mmol) in tetrahydrofuran (50 mL) was refluxed for 12 h. After cooling at room temperature, the reaction mixture was poured into water (200 mL), and the mixture was extracted with ethyl acetate (2 \times 100 mL). The combined organic layers were dried over anhydrous Na_2SO_4 . The insoluble material was filtered off, and the filtrate was concentrated under reduced pressure. The obtained residue was triturated with diethyl ether to give *tert*-butyl {2-fluoro-5-[(5-nitropyridin-2-yl)oxy]phenyl}carbamate (9.41 g, 90%) as white amorphous solid. ^1H NMR (DMSO- d_6 , 300 MHz): δ 1.51 (s, 9H), 6.73–6.79 (m, 1H), 6.81 (br s, 1H), 7.03 (d, J = 9.0 Hz, 1H), 7.13 (dd, J = 9.0, 10.5 Hz, 1H), 8.02 (d, J = 4.5 Hz, 1H), 8.47 (dd, J = 3.0, 9.0 Hz, 1H), 9.04 (d, J = 2.7 Hz, 1H).

A suspension of *tert*-butyl {2-fluoro-5-[(5-nitropyridin-2-yl)oxy]phenyl}carbamate (3.49 g, 10 mmol) and 10% palladium-carbon (1.0 g) in methanol/tetrahydrofuran (1:1, 40 mL) was vigorously stirred at room temperature under hydrogen atmosphere for 12 h. The insoluble material was filtered off, and the filtrate was concentrated under reduced pressure. The residue was poured into water (200 mL), and the mixture was extracted with ethyl acetate (2 \times 100 mL). The combined organic layers were dried over anhydrous Na_2SO_4 . The insoluble material was filtered off, and the filtrate was concentrated under reduced pressure, and the residue was triturated with diethyl ether to give **12** (3.00 g, 94%) as white amorphous solid. ^1H NMR (DMSO- d_6 , 300 MHz): δ 1.50 (s, 9H), 3.49 (br s, 2H), 6.65–6.70 (m, 1H), 6.71 (br s, 1H), 6.75 (d, J = 8.7 Hz, 1H), 7.02 (dd, J = 9.0, 10.5 Hz, 1H), 7.07 (dd, J = 3.0, 8.4 Hz, 1H), 7.68 (d, J = 3.0 Hz, 1H), 7.88 (d, J = 2.7 Hz, 1H). MS (ESI): m/z 320 (M+H) $^+$.

5.11. *tert*-Butyl {5-[(2-amino[1,3]thiazolo[5,4-*b*]pyridin-5-yl)oxy]-2-fluorophenyl}carbamate (13)

To a solution of **12** (3.00 g, 9.4 mmol) and potassium thiocyanate (3.93 g, 40 mmol) in acetic acid (40 mL) was added dropwise bromine (2.40 g, 15 mmol) under ice-cooling, and the mixture was stirred at room temperature for 12 h. The yellow insoluble material was filtered off, and the filtrate was concentrated under reduced pressure. To the residue was added saturated NaHCO_3 (200 mL), and the mixture was extracted with ethyl acetate (2 \times 100 mL). The combined organic layers were dried over anhydrous Na_2SO_4 . The insoluble material was filtered off, and the filtrate was concentrated under reduced pressure. The obtained residue was triturated with diethyl ether to give **13** (3.20 g, 90%) as pale yellow amorphous solid. ^1H NMR (DMSO- d_6 , 300 MHz): δ 1.51 (s, 9H), 5.49 (br s, 2H), 6.71–6.76 (m, 2H), 6.85 (d, J = 8.4 Hz, 1H), 7.06 (dd, J = 9.0, 10.5 Hz, 1H), 7.73 (d, J = 8.7 Hz, 1H), 8.30 (br s, 1H). HRMS (ESI): calcd for $\text{C}_{17}\text{H}_{17}\text{FN}_4\text{O}_3\text{S}$ [M+H] $^+$ 377.1078. Found: 377.1070.

5.12. *tert*-Butyl (5-{{2-(acetylamino)[1,3]thiazolo[5,4-*b*]pyridin-5-yl}oxy)-2-fluorophenyl]carbamate (14)

To a solution of **13** (1.13 g, 3.0 mmol) and DMAP (1.22 g, 10 mmol) in pyridine (10 mL) was added dropwise acetyl chloride

(0.79 g, 10 mmol) under ice-cooling, and the reaction mixture was stirred at room temperature for 12 h. To the reaction mixture was added water (200 mL), and the mixture was extracted with ethyl acetate (2 × 100 mL). The combined organic layers were dried over anhydrous MgSO₄. The insoluble material was filtered off, and the filtrate was concentrated under reduced pressure. The obtained residue was purified by silica gel column chromatography (0–100% ethyl acetate/*n*-hexane), and triturated with diethyl ether to give **14** (0.65 g, 52%) as white amorphous solid. ¹H NMR (DMSO-*d*₆, 300 MHz): δ 1.52 (s, 9H), 2.24 (s, 3H), 6.76–6.80 (m, 1H), 6.81–6.89 (m, 1H), 6.97 (dd, *J* = 4.5, 8.7 Hz, 1H), 7.09 (dd, *J* = 9.0, 10.5 Hz, 1H), 7.93 (d, *J* = 8.7 Hz, 1H), 7.98 (br s, 1H), 10.45 (br s, 1H). MS (ESI): *m/z* 419 (M+H)⁺.

5.13. Mechanism analysis of Boc introducing reaction of **1**

To a mixture of compound **1** (300 mg, 0.547 mmol) and pyridine (0.88 mL, 10.9 mmol) in tetrahydrofuran (2.12 mL) was added di-*tert*-butyl dicarbonate (119 mg, 0.545 mmol) at room temperature. The reaction mixture was stirred at room temperature. During the reaction, test samples (50 μL) of the reaction mixture were taken out at 1, 30, 60, 160 min. Then, additional amount of di-*tert*-butyl dicarbonate (119 mg, 0.545 mmol) was added at room temperature. During the further reaction, test samples (50 μL) of the reaction mixture were taken out at additional 30 and 60 min. The final di-*tert*-butyl dicarbonate (119 mg, 0.545 mmol) was added to the reaction mixture. The mixture was stirred at room temperature for additional 30 min, and 50 μL of the reaction mixture was sampled at 30 min. To the reaction mixture was added 1 N HCl (15 mL) and 1,2-dimethoxyethane (15 mL) at room temperature. The mixture was stirred at room temperature, and sampled at 2 h after 1 N HCl addition. The reaction mixture was warming up to 35 °C and stirred at 35 °C for 2 h, then sampled. The volume of each samples was 50 μL. The sampled mixture was partitioned between ethyl acetate (1.0 mL) and water (0.2 mL). Ethyl acetate layer was sampled (0.7 mL), and evaporated under reduced pressure. The resulting oily residue was analyzed by TLC (ethyl acetate/*n*-hexane = 1:1) and ¹H NMR spectroscopy.

5.14. In vitro hydrolysis test

In vitro hydrolysis stability of compound **6b** was tested using hepatic microsomes obtained from rats, dogs, monkeys and humans (Table 5). The incubation mixtures were prepared under ice-cold conditions by adding 20 μL of the microsomes (4 mg protein/mL), 50 μL of potassium phosphate buffer (50 mmol/L, pH 7.4) and 29 μL of ultrapure water in an eppendorf tube. The reactions were initiated by adding 1 μL of compound solution (10 μmol/L) to the incubation mixtures. Incubations were conducted at 37 °C for 2 h and terminated by adding 100 μL of the ice-cold acetonitrile. The zero-time incubations which served as the controls were terminated by adding the ice-cold acetonitrile before adding compound. The samples were mixed by vortex mixing vigorously and centrifuging at 3000×*g* for 10 min at 4 °C. The supernatant fractions were subjected to high performance liquid chromatography (HPLC) with an UV detector. All incubations were made in duplicate.

In vitro hydrolysis stability of compound **1** and **2** was tested using incubation mixture (1 mg protein/mL) and compound solution (30 μmol/L) (Table 1). Incubations were conducted at 37 °C for 60 min.

5.15. Powder X-ray diffractometry (XRD)

Powder X-ray diffraction patterns were collected using a RINT 2100 Ultima+ (Rigaku, Tokyo, Japan) with Cu Kα ($\lambda = 1.5418 \text{ \AA}$)

radiation generated at 50 mA and 40 kV. Sample was placed on silicone plate at room temperature. Data was collected from 2° to 35° (2θ) at a step size of 0.02° and scanning speed of 6°/min. The crystallinity of each sample was calculated by Hermans method.¹⁹ The procedure is described as follows: (1) calculate all peak areas from the XRD pattern of the sample; (2) subtract background area from the area of (1) by the blank analysis; (3) subtract the halo pattern derived from amorphous in the sample from the area of (2); (4) calculate the crystallinity of the sample, [Area of 3]/[Area of 2] × 100.

5.16. Thermal analysis

Differential scanning calorimetry (DSC) was performed using a DSC EXSTAR 6200 system (Seiko Instruments, Chiba, Japan). A DSC thermogram was obtained in a closed aluminum pan using a sample weight of ca 3 mg and a heating rate of 5 °C/min under a nitrogen flow at 50 mL/min.

5.17. Thermodynamic solubility

About 0.5 mg of sample was added to 0.5 mL of a dissolving solvents, which was 20 mmol/L bile acid in the JP 2nd fluid for disintegration solution (pH 6.8)¹⁶, and the sample solution were shaken at 37 °C for 18 h. The solution was filtered through a membrane filter (0.45 μm). The filtrate was diluted with acetonitrile and analyzed by high-performance liquid chromatography (HPLC). The sample solutions were analyzed with an HPLC system (W2695, Waters, Milford, MA, USA) and UV detector (W2487, Waters) operated at 230 nm. The packaged column was Shiseido MG-III ODS (3 μm, 4.6 × 75 mm, Shiseido, Tokyo, Japan) operated at 40 °C at a flow rate of 1.0 mL/min. The two mobile phases used were (A) 50 mmol/mL ammonium acetate buffer and (B) acetonitrile. The elution program started at 100:0 = A:B, ramped linearly to 0:100 = A:B at 5 min, held there until 7 min, and returned to 100:0 = A:B at 8 min.

5.18. Intrinsic dissolution rate

The initial dissolution rates were measured using rotating disk method.²⁰ About 20 mg of drug substance was compressed at the force of 20 kN/cm² using a single tablet punch press to obtain a 7 mm diameter disk. The solvent for the dissolution test was 250 mL of 200 mmol/L bile acid in the JP 2nd fluid for disintegration solution (pH 6.8).¹⁶ The disk was rotated at 200 rpm at 37 °C. At each time interval a 0.50 mL portion of an aliquot of the solution was withdrawn from the flask and diluted with acetonitrile to provide twice diluted solution. The compound concentration was analyzed by HPLC.

5.19. X-Ray crystallographic analysis.¹⁷

A single crystal (0.14 × 0.08 × 0.04 mm) of ethanol cocrystal **6a** was obtained by recrystallization from ethanol. A single crystal (0.24 × 0.15 × 0.08 mm) of acetic acid cocrystal **6b** was obtained by recrystallization from acetic acid. All measurements were made on a Rigaku R-Axis RAPID diffractometer using graphite monochromated Cu-Kα radiation. The structures were solved by direct methods using the program SIR92.²¹ The structures were then refined by the full-matrix least-squares refinement (SHELXL97²²) with anisotropic temperature factors for the non-hydrogen atoms and isotropic temperature factors for the hydrogen atoms. Crystal data for **6a**; C₃₂H₂₇ClFN₅O₅S·C₂H₅OH; *M* = 694.18; triclinic, space group P-1 (#2), *a* = 9.1155(2), *b* = 12.7039(2), *c* = 15.2671(3) Å, α = 96.0441(7), β = 107.4964(7), γ = 93.7673(7)°, *V* = 1667.94(6) Å³, *Z* = 2, *D*_c = 1.382 g/cm³, *R*₁ = 0.051, *wR*₂ = 0.172 for 3606 observed reflections with *I* > 2σ (*I*). Crystal data for **6b**; C₃₂H₂₇ClFN₅O₅S·C₂H₄O₂; *M* = 708.16; triclinic, space group P-1

(#2), $a = 9.158(4)$, $b = 13.669(6)$, $c = 13.891(6)$ Å, $\alpha = 91.75(3)$, $\beta = 92.17(3)$, $\gamma = 96.83(3)^\circ$, $V = 1724(4)$ Å³, $D_c = 1.364$ g/cm³, $Z = 2$, $R1 = 0.076$, $wR2 = 0.168$ for 3032 observed reflections with $1.2\sigma(I)$.

5.20. In vivo xenograft model

All experiments were approved by the Takeda Animal Care and Use Committee (Approved No.: TEACUC-00004191, TEACUC-2719). Human melanoma cell line A375 (purchased from American Type Culture Collection (ATCC)) was proliferated in Dulbecco's modified Eagle medium (DMEM) (Invitrogen) supplemented with 10% heat-inactivated fetal bovine serum. The cells were cultured in tissue culture dishes in a humidified incubator at 37 °C in an atmosphere of 5% CO₂. Compound **6b** was suspended in vehicle solution including 0.5% methylcellulose (Shin-Etsu Chemical) solution. Six-week old female athymic nude rats (F344/N Jcl-rnu/rnu female (CLEA Japan, Inc.)) were received subcutaneous injections with 3×10^6 A375 cells in 100 µL of Hanks' balanced salt solution (Invitrogen). When tumors reached a volume of 150–250 mm³, mice were orally administrated with vehicle or compound **6b** (12.9, 32.3, 64.6 and 129 mg/kg). At 4 h after administration, the tumor was collected and homogenized in the lysis buffer (1% NP-40, 0.5 % sodium deoxycholate, 1 % SDS, 97.5 % Dulbecco's phosphate-buffered salines (DPBS) (GIBCO) with Protease Inhibitor Cocktail Set 3 (Calbiochem) and Phosphatase Inhibitor Cocktail 2 (Sigma)). The protein concentration in the tumor lysate was determined by bicinchoninic acid (BCA) protein assay kit (Thermo), and adjusted to 1.25 µg/µL. An equal volume of 2× SDS sample buffer (BioRad) was added to the above-mentioned protein solution and incubated at 95 °C for 5 min. The cell lysates were applied to SDS-PAGE, and the protein was transferred onto Sequi-Blot™ polyvinylidene difluoride (PVDF) membrane with the iBlot™ Dry Blotting System (Invitrogen). The cells membrane were blocked with the Starting Block Blocking Buffer (PIERCE), and reacted overnight with anti-phosphorylated ERK1/2 (Ser217/221) (Cell signaling) diluted 1000-fold with Can Get Signal® Immunoreaction Enhancer Solution I (TOYOBO). The membrane was washed with TBS containing 0.05% Tween 20 (Wako Pure Chemical Industries, Ltd.), and reacted at room temperature for 1 h with horseradish peroxidase (HRP) labeled rabbit IgG polyclonal antibody (GE Healthcare) diluted 2000-fold with Can Get Signal® Immunoreaction Enhancer Solution II (TOYOBO). The membrane was washed in the same manner as above, chemical luminescence of a phosphorylated MEK1/2 protein labeled with the antibody, which was caused by ECL-plus Detection Reagent (GE Healthcare), was detected by Luminescent Image Analyzer LAS-1000 (FUJIFILM Corporation). Taking the luminescence of the control group free of the test compound as 100%, the concentration (IC₅₀ value) of the compound necessary for inhibiting the residual luminescence to 50% of the control group was calculated using PCP software (SAS Institute). For tumor growth experiments, rats were randomized into 5 groups ($n = 4$) and orally administrated with vehicle or compound **6b** (12.9, 32.3, 64.6 and 129 mg/kg) twice-daily for two weeks. Tumor volumes were calculated as $\text{volume} = L \times l^2 \times 1/2$, where L was taken to be the longest diameter across the tumor and l the corresponding perpendicular. Treatment over control ($T/C, \%$), an index of anti-tumor efficacy, was calculated by comparison of the mean change in tumor volume over the treatment period for the control and treated groups. Body weight was also measured on the day of tumor volume assessment.

5.21. Pharmacokinetic studies

For oral cassette dosing PK study, test compounds were dissolved in a mixture of DMSO and 1,3-butylene glycol and were

administered orally to non-fasted mice at a dose of 10 mg/kg. For single dosing PK study of **6b**, the compound was suspended in 0.5% methylcellulose solution for oral administration. Blood samples were taken from the femoral vein at the designated time points after dosing, and centrifuged to obtain the plasma fractions. The plasma samples were de-proteinized with acetonitrile containing an internal standard. After centrifugation, the supernatant was diluted with a mixture of 0.01 mol/L ammonium formate solution and acetonitrile (9:1, v/v) and centrifuged again. The compound concentrations in the supernatant were measured by LC/MS/MS.

Acknowledgments

The authors would like to thank Yukiko Watanabe for her assistance in PK evaluation. The authors would like to thank Yoichi Nagano for his assistance in crystallographic data deposition to the Cambridge Crystallographic Data Centre.

Supplementary data

Supplementary data associated with this article can be found, in the online version, at <http://dx.doi.org/10.1016/j.bmc.2012.06.015>. These data include MOL files and InChIKeys of the most important compounds described in this article.

References and notes

- Okaniwa, M.; Hirose, M.; Imada, T.; Ohashi, T.; Hayashi, Y.; Miyazaki, T.; Arita, T.; Yabuki, M.; Kakoi, K.; Kato, J.; Takagi, T.; Kawamoto, T.; Yao, S.; Sumita, A.; Tsutsumi, S.; Tottori, T.; Oki, H.; Sang, B.-C.; Yano, J.; Aertgeerts, K.; Yoshida, S.; Ishikawa, T. *J. Med. Chem.* **2012**, *55*, 3452.
- Janssens, S.; Van den Mooter, G. *J. Pharm. Pharmacol.* **2009**, *61*, 1571.
- Ettmayer, P.; Amidon, G. L.; Clement, B.; Testa, B. *J. Med. Chem.* **2004**, *47*, 2393.
- Kerns, E.; Di, L. In *Drug-like properties Concepts, structure design and methods from ADME to toxicity optimization*; Academic Press Inc., 2008; Vol. 39, pp. 426–438.
- Stella, V. J.; Nti-Addae, K. W. *Adv. Drug Deliv. Rev.* **2007**, *59*, 677.
- Férriz, J. M.; Vinšová, J. *Curr. Pharm. Des.* **2010**, *16*, 2033.
- Beaumont, K.; Webster, R.; Gardner, I.; Dack, K. *Curr. Drug Metab.* **2003**, *4*, 461.
- Schultz, C. *Bioorg. Med. Chem.* **2003**, *11*, 885.
- Ishikawa, T.; Matsunaga, N.; Tawada, H.; Kuroda, N.; Nakayama, Y.; Ishibashi, Y.; Tomimoto, M.; Ikeda, Y.; Tagawa, Y.; Iizawa, Y.; Okonogi, K.; Hashiguchi, S.; Miyake, A. *Bioorg. Med. Chem.* **2003**, *11*, 2427.
- Ikeda, Y.; Ban, J.; Ishikawa, T.; Hashiguchi, S.; Urayama, S.; Horibe, H. *Chem. Pharm. Bull.* **2008**, *56*, 1406.
- Krise, J. P.; Zygmunt, J.; Georg, G. I.; Stella, V. J. *J. Med. Chem.* **1999**, *42*, 3094.
- Hemenway, J. N.; Stella, V. J. *J. Pharm. Sci.* **2010**, *99*, 4565.
- Shaw, K. J.; Erhardt, P. W.; Hagedorn, A. A.; Ill; Pease, C. A.; Ingebretsen, W. R.; Wiggins, J. R. *J. Med. Chem.* **1992**, *35*, 1267.
- Kerns, E.; Di, L. In *Drug-like properties: Concepts, structure design and methods from ADME to toxicity optimization*; Academic Press Inc., 2008; Vol. 7, pp. 56–85.
- International Conference on Harmonization of Technical Requirements for Registration of Pharmaceuticals for Human Use. Impurities: Guideline for residual solvents. Q3C(R4). February 2009.
- The Ministry of Health, Labour and Welfare Ministerial Notification No. 285, <http://jpub.nihs.go.jp/jp15e/>, General tests/reagents, test solutions. The Japanese pharmacopoeia English version, 2006, 15, pp. 239.
- CCDC 862986 (6a) and CCDC 863435 (6b) contain the supplementary crystallographic data for this paper. These data can be obtained free of charge from The Cambridge Crystallographic Data Centre via www.ccdc.cam.ac.uk/data_request/cif.
- Allen, F. H.; Kennard, O.; Watson, D. G. *J. Chem. Soc., Perkin Trans. II* **1987**, S1.
- Hermans, P. H.; Weidinger, A. *J. Appl. Phys.* **1948**, *19*, 491.
- Terada, K.; Kitano, H.; Yoshihashi, Y.; Yonemochi, E. *Pharm. Res.* **2000**, *17*, 920.
- Altomare, A.; Cascarano, G.; Giacobozzo, C.; Guagliardi, A.; Burla, M. C.; Polidori, G.; Camalli, M. *J. Appl. Cryst.* **1994**, *27*, 435.
- Sheldrick, G. M. SHELXL97. Program for the refinement of crystal structures. University of Göttingen, Germany, 1997.